

Published in final edited form as:

*Nat Med.* 2011 January ; 17(1): 25–29. doi:10.1038/nm0111-25.

## Lack of HIF-2 $\alpha$ in limb bud mesenchyme causes a modest and transient delay of endochondral bone development

Elisa Araldi<sup>1</sup>, Richa Khatri<sup>1</sup>, Amato J Giaccia<sup>2</sup>, M Celeste Simon<sup>3</sup>, and Ernestina Schipani<sup>1</sup>

Ernestina Schipani: schipani@helix.mgh.harvard.edu

<sup>1</sup>Endocrine Unit, Department of Medicine, Massachusetts General Hospital–Harvard Medical School, Boston, Massachusetts, USA

<sup>2</sup>Division of Cancer and Radiation Biology, Department of Radiation Oncology, Stanford University School of Medicine, Stanford, California, USA

<sup>3</sup>Abramson Family Cancer Research Institute, University of Pennsylvania School of Medicine, Philadelphia, Pennsylvania, USA

### To the Editor

Two papers recently published in *Nature Medicine* provide evidence that hypoxia-inducible factor-2 $\alpha$  (HIF-2 $\alpha$ ) is crucial for articular surface homeostasis through mechanisms that involve, at least in part, regulation of genes such as *Col10a1* (encoding the  $\alpha$ 1 chain of type X collagen, Col10A1), *Mmp13* (encoding matrix metallo-proteinase-13, MMP-13) and *Vegfa* (encoding vascular endothelial growth factor-A, VEGF)<sup>1,2</sup>. Interestingly, Saito *et al.*<sup>1</sup> also report a mild delay of chondrocyte hypertrophy in fetal growth plates of mice heterozygous for genetic knockout of HIF-2 $\alpha$  (encoded by *Epas1*). The key implication of this finding is that homozygous loss of HIF-2 $\alpha$  would markedly delay chondrocyte hypertrophy and replacement of cartilage by bone. However, as shown below, we found that this was not the case.

HIF-2 is a heterodimer of two proteins, HIF-2 $\alpha$  and HIF-1 $\beta$ <sup>3</sup>. HIF-1 $\beta$  is constitutively expressed, whereas HIF-2 $\alpha$  is the hypoxia-responsive component of the complex. The other HIF- $\alpha$  isoform is HIF-1 $\alpha$ . Both isoforms are regulated by oxygen in a similar fashion. However, the two  $\alpha$  subunits partially differ in their biological functions and in their molecular targets<sup>3</sup>.

The vast majority of skeletal bones are derived from the replacement of a chondrocyte mold by bone tissue according to a well-defined temporal and spatial sequence of events<sup>4,5</sup>. Undifferentiated mesenchymal cells condense and become highly proliferating chondrocytes. Proliferative chondrocytes synthesize type II collagen (Col2A1) and form a columnar layer; they then stop proliferating and differentiate into postmitotic hypertrophic cells. Hypertrophic chondrocytes predominantly synthesize Col10A1 and mineralize their surrounding matrix. This unique differentiation process, which is called endochondral bone development, is followed by death of hypertrophic chondrocytes, blood vessel invasion and, finally, replacement of the cartilaginous matrix with bone. HIF-1 has an essential and nonredundant role in endochondral bone development<sup>4,5</sup>.

© 2011, Nature America, Inc. All rights reserved.

Note: Supplementary information is available on the Nature Medicine website.

#### COMPETING FINANCIAL INTERESTS

The authors declare no competing financial interests.

To unequivocally prove a role for HIF-2 $\alpha$  in fetal cartilage development and particularly in chondrocyte hypertrophy, we conditionally inactivated HIF-2 $\alpha$  in limb bud mesenchyme using a *Prx1* promoter– driven Cre–transgenic mouse and a mouse homozygous for a floxed *Epas1* allele (*Epas1*<sup>fl/fl</sup>) or a double heterozygote for a floxed *Epas1* allele and a universal null *Epas1* allele (*Epas1*<sup>fl/-</sup>), respectively. Each of the three mouse lines has been extensively characterized and used in previous studies<sup>5</sup>.

At birth and throughout their weaning period, *Prx1*-Cre; *Epas1*<sup>fl/fl</sup> and *Prx1*-Cre; *Epas1*<sup>fl/-</sup> mutant mice looked indistinguishable from *Prx1*-Cre; *Epas1*<sup>fl/+</sup>, *Prx1*-Cre; *Epas1*<sup>+/-</sup> and *Epas1*<sup>fl/fl</sup> control mice (data not shown). PCR analysis of genomic DNA extracted from newborn *Prx1*-Cre; *Epas1*<sup>fl/fl</sup> and control chondrocytes showed that recombination of the *Epas1* in mutant chondrocytes was virtually complete (Supplementary Fig. 1a). In addition, accumulation of HIF-2 $\alpha$  protein was severely decreased in embryonic day 15.5 (E15.5) *Prx1*-Cre; *Epas1*<sup>fl/-</sup> hindlimb paws when compared to controls (Supplementary Fig. 1b); the very modest residual signal observed in mutant specimens was probably the result of background staining.

Whole-mount alizarin red S and alcian blue staining of mutant skeletons at birth revealed no pattern defect and no difference in length of the long bones when compared to control specimens (Fig. 1a). BrdU analysis performed at E15.5 did not show any change of chondrocyte proliferation rate in growth plates lacking HIF-2 $\alpha$  (Supplementary Fig. 1c); moreover, we did not observe any difference in TUNEL staining in mutants versus controls (data not shown).

We then pursued a systematic analysis of tibias and paws at various stages of fetal and postnatal development by routine histology and *in situ* hybridization. E13.5 mutant paws were histologically indistinguishable from controls; in particular, the appearance of *Col10a1* mRNA–expressing cells was not delayed by loss of HIF-2 $\alpha$  (Fig. 1b and data not shown). These findings indicate that HIF-2 $\alpha$  is dispensable for mesenchymal condensations, for differentiation of mesenchymal cells into chondrocytes and for *Col10a1* mRNA expression, at least at early stages of cartilage formation. Of note, during endochondral bone development, accumulation of detectable levels of *Col10a1* mRNA consistently preceded the appearance of hypertrophic chondrocytes (Fig. 1b).

At E15.5, mutant tibia length was comparable to control (Fig. 1c and data not shown), as was extension of the domain of expression of *Col2a1* mRNA in the growth plate, whereas the extension of the domain of expression of *Col10a1* mRNA and, in particular, of the subdomain expressing osteopontin (*Spp1*), *Mmp13* and *Vegfa* mRNAs, was shorter in mutants, although the difference was statistically significant only for the subdomain (Fig. 1c and data not shown). Osteopontin, MMP13 and VEGF are produced by late hypertrophic cells; that is, by those chondrocytes whose appearance immediately precedes blood vessel invasion and replacement of cartilage by bone. All in all, our findings thus indicate that, whereas appearance of *Col10a1* mRNA–expressing cells is not affected by loss of HIF-2 $\alpha$ , as shown by analysis of E13.5 hindlimb paw, differentiation of hypertrophic, *Col10a1* mRNA–producing cells into late hypertrophic cells expressing *Col10a1*, *Spp1*, *Mmp13* and *Vegfa* mRNAs is modestly, though significantly, impaired by lack of this transcription factor.

Consistent with these data, E17.5 mutant tibias were slightly shorter than controls; moreover, the distance between the two *Col10a1* mRNA domains and, thus, the extension of the bone marrow cavity, were modestly decreased (Fig. 1d), features that were all probably consequences of the delayed appearance of late hypertrophic chondrocytes and, therefore, of the delayed replacement of cartilage by bone. Of note, however, none of these differences

reached statistical significance, which highlights the overall extremely modest nature of the phenotype in the mutants. Indeed, postnatally, mutants and controls were virtually indistinguishable, as shown by whole-mount alizarin red S and alcian blue staining, routine histology and *in situ* hybridization (Fig. 1a, **Supplementary** Fig. 1d and data not shown).

In summary, differently from what we might have predicted on the basis of the findings in *Epas1*<sup>+/-</sup> mice reported by Saito *et al.*<sup>3</sup>, homozygous loss of HIF-2 $\alpha$  in limb bud mesenchyme achieved by conditional knockout causes only a modest delay of endochondral bone development. More important, differently from what Saito *et al.*<sup>3</sup> suggests, this delay is not due to impairment of Col10A1 accumulation, as Col10A1 expression is very robust and occurs in a timely manner in growth plates lacking HIF-2 $\alpha$ , but rather is secondary to a very modest impairment of differentiation of hypertrophic cells into late hypertrophic chondrocytes. Last, the delay of endochondral bone development in mutants is transient and no longer detectable in postnatal life.

In conclusion, the role of HIF-2 $\alpha$  in growth plate development and, particularly, in expression of *Col10a1* mRNA, is not as crucial as it is in articular surface homeostasis. Identification of the molecular and cellular mechanisms responsible for this difference requires further studies.

## Acknowledgments

This paper was supported by US National Institutes of Health grant RO1 AR048191-06 to E.S.

## References

1. Saito T, et al. Nat Med. 2010; 16:678–686. [PubMed: 20495570]
2. Yang S, et al. Nat Med. 2010; 16:687–693. [PubMed: 20495569]
3. Gordon JD, Simon M. Curr Opin Genet Dev. 2007; 17:71–77. [PubMed: 17208433]
4. Araldi E, Schipani E. Bone. 2010; 47:190–196. [PubMed: 20444436]
5. Provot S, et al. J Cell Biol. 2007; 177:451–464. [PubMed: 17470636]

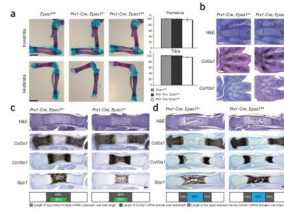


**Figure 1.**

Phenotypic analysis of *Prx1*-Cre; *Epas1*<sup>fl/fl</sup> and control littermates in embryonic and neonatal stages. **(a)** Whole-mount alizarin red S and alcian blue staining of hindlimb and forelimb zeugopods and stylopods isolated from newborn mutant and control mice. Scale bar, 1 mm. Length of tibia and humerus is shown as percentage of *Epas1*<sup>fl/fl</sup> controls  $\pm$  s.d. The bar graph is a quantification of the data in the images. Differences between mutants and controls are not statistically significant. **(b)** H&E staining and *in situ* hybridization analysis of E13.5 mutant and control autopods. Bright-field images are shown. Scale bars: 100  $\mu$ m (top) and 200  $\mu$ m (bottom two rows). **(c)** H&E staining and *in situ* hybridization analysis of E15.5 mutant and control tibias. Bright-field images of one representative experiment are shown. Scale bar, 100  $\mu$ m. Lengths of *Col10a1* mRNA subdomains and of *Col10a1/Spp1/Mmp13/Vegfa* mRNAs subdomains are expressed as percentage of specimen total length (bottom). The difference in length between the mutant subdomain expressing *Col10a1*, *Spp1*, *Mmp13* and *Vegfa* mRNAs and control (bottom) is statistically significant ( $P < 0.05$ ). **(d)** H&E staining and *in situ* hybridization analysis of E17.5 mutant and control tibias. Bright-field images of one representative experiment are shown. Scale bar, 200  $\mu$ m. Lengths of *Col10a1* mRNA subdomains and distance between the two *Col10a1* mRNA domains are expressed as percentage of specimen total length (bottom); differences in length between mutants and controls are not statistically significant.